Am J Nucl Med Mol Imaging 2026;16(5):196-201
www.ajnmmi.us /ISSN:2160-8407/ajnmmi0171876

Case Report

^{18}F-FDG PET/CT evaluation of primary renal Ewing sarcoma/primitive neuroectodermal tumor: a case report and literature review

Jin Jiang*, Yongkang Qiu*, Tingting Yuan, Zhao Chen, Hongwei Sun, Lei Kang

*Department of Nuclear Medicine, Peking University First Hospital, Beijing 100034, China. *Equal contributors.*

Received February 3, 2026; Accepted September 7, 2026; Epub October 15, 2026; Published October 30, 2026

Abstract: Primary renal Ewing sarcoma/primitive neuroectodermal tumor (ES/PNET) is rare, and few reports have described serial ^{18}F-FDG PET/CT findings. A 34-year-old man presented with a 20-cm mixed cystic-solid mass in the right kidney. Baseline PET/CT showed intense FDG uptake in the solid component, with a maximum standardized uptake value (SUVmax) of 23.8 at 62 minutes and 32.7 at 120 minutes; no distant FDG-avid lesions were identified. Core needle biopsy and detection of an *EWSR1-FLI1* rearrangement established the diagnosis. After individualized systemic treatment and radical right nephrectomy, serial CT showed no definite progression. At 21 months after surgery, PET/CT showed nodular FDG uptake in the surgical bed (SUVmax 9.7 at 66 minutes and 11.4 at 186 minutes). Local recurrence could not be excluded, but CT showed no discrete progressively enhancing mass and subsequent imaging showed only limited change. PET/CT was useful for baseline staging and follow-up, but postoperative FDG uptake required correlation with contrast-enhanced CT and serial imaging rather than interpretation by SUV alone.

Keywords: Ewing sarcoma, primitive neuroectodermal tumor, kidney, ^{18}F-FDG PET/CT, postoperative surveillance

Introduction

Primary renal Ewing sarcoma/primitive neuroectodermal tumor (ES/PNET) is a rare extraskeletal tumor in the Ewing sarcoma family. It occurs mainly in adolescents and young adults and often presents as a large renal mass with nonspecific symptoms and imaging findings [1-4]. Because its imaging appearance overlaps with that of other renal tumors, diagnosis relies on histopathology, immunohistochemistry, and molecular evidence of an *EWSR1* rearrangement involving an ETS-family partner [1, 5, 6].

^{18}F-fluorodeoxyglucose positron emission tomography/computed tomography (^{18}F-FDG PET/CT) is used for staging and follow-up in Ewing sarcoma. It provides whole-body assessment, particularly for bone metastases, and can detect recurrent or metastatic disease [7-10]. Its role in primary renal ES/PNET is less well defined because published data are limited. Case reports have described FDG-avid primary tumors, venous tumor thrombi, lymph node metastases, and distant metastases [11-15].

We report serial PET/CT and CT findings in a patient with primary renal ES/PNET, with particular attention to baseline staging and the interpretation of postoperative FDG uptake.

Case presentation

In February 2023, a 34-year-old man presented with new-onset hypertension and right upper abdominal pain. Evaluation revealed a right renal mass. His blood pressure was 160/100 mmHg, and his Eastern Cooperative Oncology Group performance status was 0. Routine serum tumor markers, including carcinoembryonic antigen, carbohydrate antigen 19-9, carbohydrate antigen 72-4, and carbohydrate antigen 242, were negative on repeated testing. Ultrasonography showed a large mixed cystic-solid mass in the right kidney, and ^{18}F-FDG PET/CT was performed for whole-body staging.

After fasting, 278 MBq (7.5 mCi) of ^{18}F-FDG was administered intravenously. Standard torso and brain PET/CT imaging began 62 minutes after injection; delayed imaging was obtained at 120 minutes, 58 minutes after the start of standard imaging. PET/CT showed a 13 × 12 × 20 cm mixed cystic-solid mass centered in the right kidney. The solid component showed intense FDG uptake, with a maximum standardized uptake value (SUVmax) of 23.8 on standard imaging and 32.7 on delayed imaging (**Figure 1**). The mass had poorly defined margins, and involvement of the adjacent right adrenal gland, right psoas muscle, abdominal wall, peritoneum, and right renal vein could not be excluded. No distant FDG-avid lesion was identified.

Ultrasound-guided core needle biopsy was performed on February 20, 2023. Histopathology showed a small round cell sarcoma with patchy necrosis (**Figure 2A** and **2B**). The tumor was strongly positive for vimentin and synaptophysin and positive for desmin, with a Ki-67 index of approximately 30-50% (**Figure 2E** and **2F**). Epithelial markers, PAX8, GATA3, WT1, leukocyte common antigen, chromogranin A, CD56, HMB45, myogenin, and TLE1 were negative. Molecular testing detected an

https://doi.org/10.62347/QQOQ1162

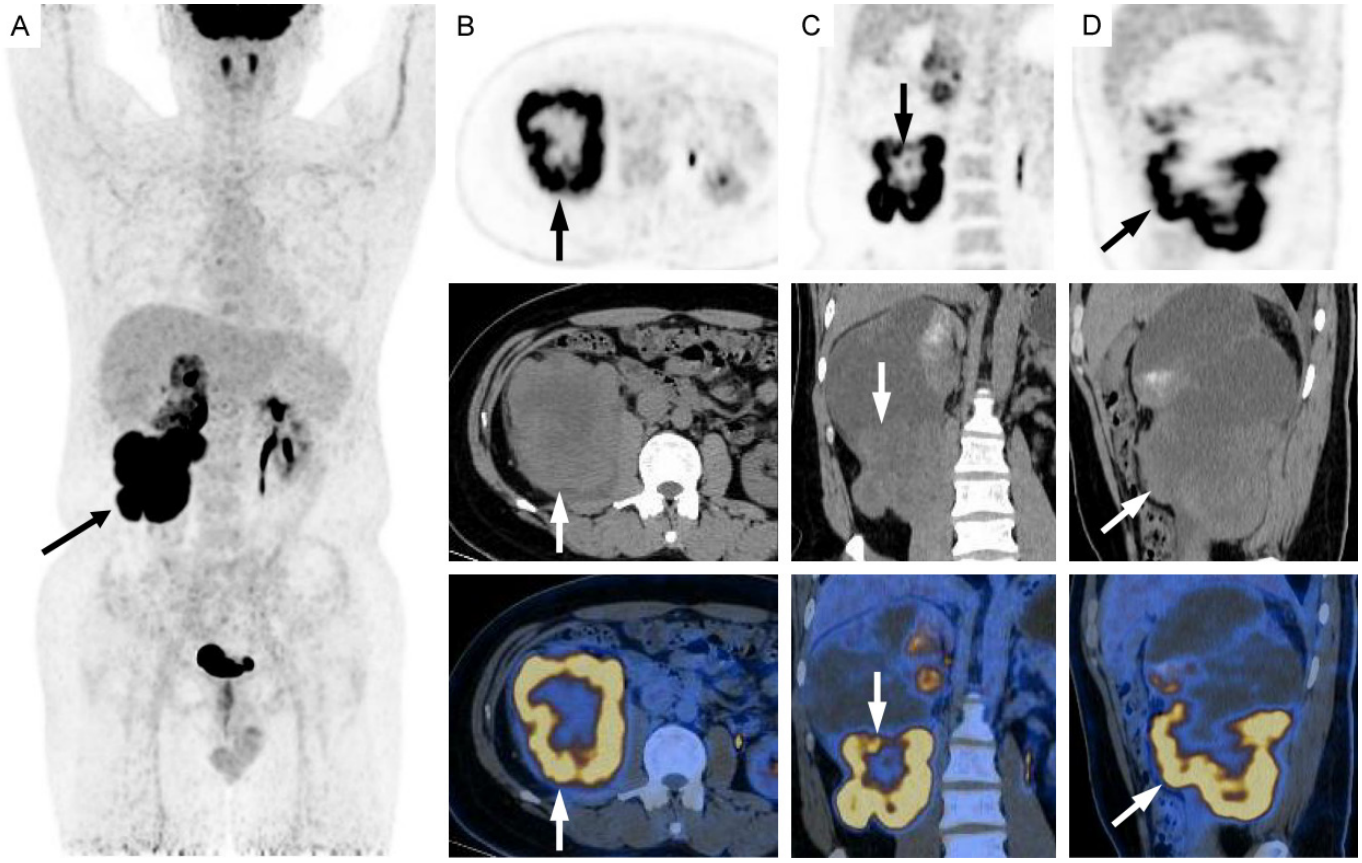


Figure 1. Initial staging imaging at diagnosis. Initial ^{18}F-FDG PET/CT shows a large, intensely FDG-avid mixed cystic-solid mass centered in the right kidney, without distant FDG-avid disease. (A) Coronal maximum intensity projection image shows the primary lesion (arrow). (B) Axial, (C) coronal, and (D) sagittal PET/CT images show the extent of the mass and intense uptake in its solid component (SUVmax 23.8 on standard imaging). SUVmax, maximum standardized uptake value.

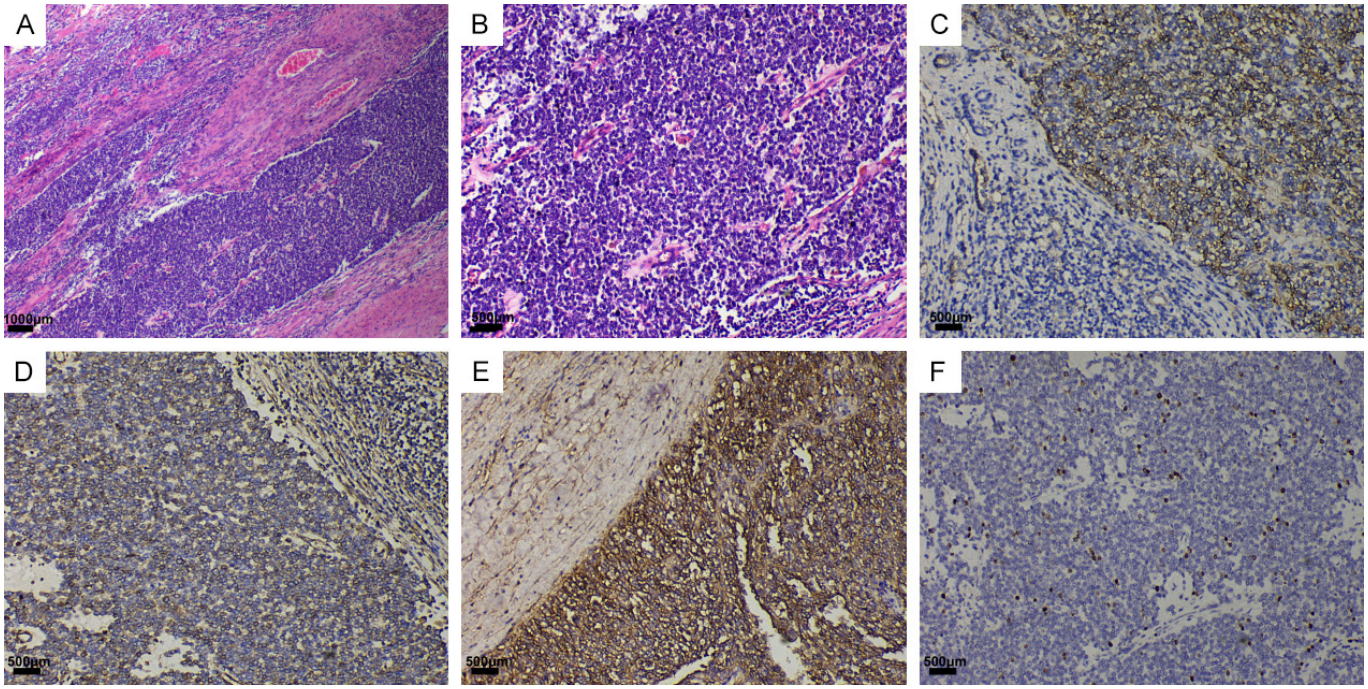


Figure 2. Histopathological and immunohistochemical findings. A. Pretreatment core biopsy, hematoxylin and eosin (H&E), 40×, shows a small round cell sarcoma. B. At 100× magnification, the tumor cells have scant cytoplasm, round nuclei, and fine chromatin. C. The postoperative resection specimen shows membranous CD99 positivity. D. Ki-67 staining in the postoperative specimen shows a proliferation index of approximately 5-10%. E. Pretreatment biopsy shows synaptophysin positivity. F. Pretreatment biopsy shows strong vimentin positivity.

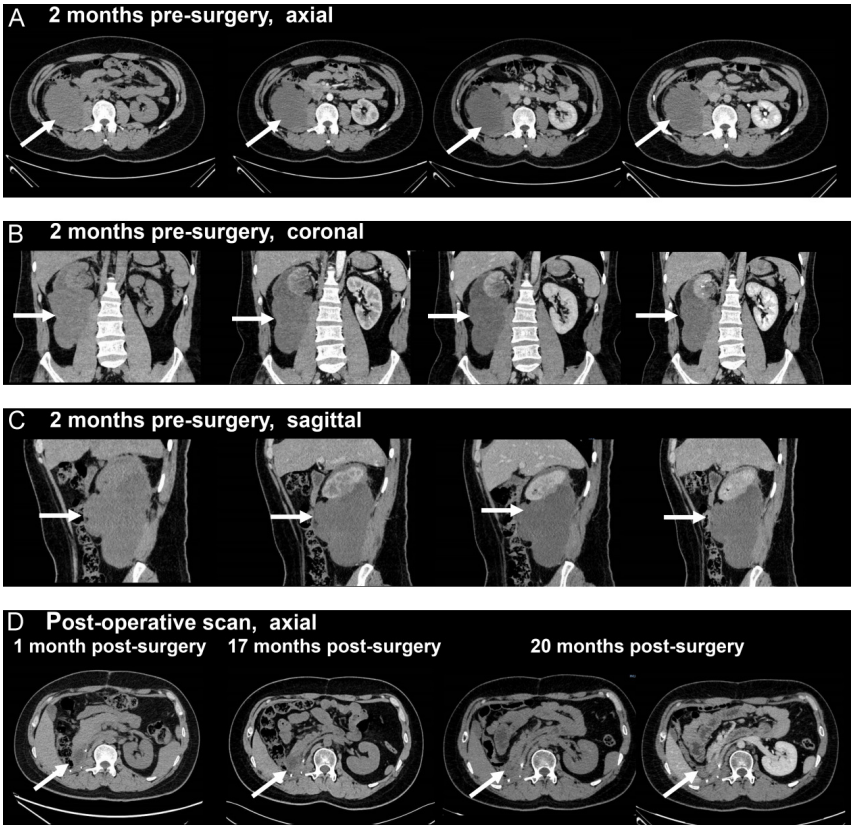


Figure 3. Multiphasic CT for treatment response assessment and follow-up. Multiphasic contrast-enhanced CT images obtained after preoperative systemic treatment and approximately 2 months before surgery are shown in axial (A), coronal (B), and sagittal (C) planes. Each series includes non-contrast, arterial, venous, and delayed phases and shows a reduction in tumor size and solid components. (D) Postoperative follow-up images are shown in order: non-contrast CT at 1 month after surgery, non-contrast CT at 17 months, and non-contrast and venous-phase CT at 20 months. Persistent soft tissue is present in the surgical bed, without a clearly enlarging or progressively enhancing mass.

EWSR1-FLI1 rearrangement, supporting the diagnosis of ES/PNET.

From April 11 to June 16, 2023, the patient received four cycles of albumin-bound paclitaxel 300 mg, carboplatin 300 mg, bevacizumab 400 mg, and sintilimab 200 mg. Multiphasic contrast-enhanced CT on May 26 showed a marked reduction in the size of the right renal and perirenal retroperitoneal mass, with a smaller solid component and less compression of adjacent structures (**Figure 3A-C**).

On August 18, 2023, the patient underwent radical right nephrectomy and retroperitoneal tumor resection. The resection specimen contained an 11 × 9 × 8 cm poorly differentiated tumor with extensive necrosis. The tumor involved the renal parenchyma and extended into the renal pelvis; the surgical margins were negative. Immunohistochemistry showed CD99 positivity, focal WT1 positivity, partial CD57 positivity, and a Ki-67 index of approximately 5-10% (**Figure 2C** and **2D**). Together with the pretreatment morphology and *EWSR1-FLI1* rearrangement, these findings supported a postoperative diagnosis of primary renal ES/PNET.

From September 12 to November 10, 2023, the patient received four postoperative cycles of eribulin 2 mg on days 1 and 8, nedaplatin 100 mg on day 1, and sintilimab 200 mg. Radiotherapy to the renal bed and elective retroperitoneal region was given from November 29, 2023, to January 3, 2024, at a dose of 50 Gy in 25 fractions over 5 weeks. During and after radiotherapy, sintilimab was continued, with intermittent oral etoposide 100 mg daily for 10 days in a 21-day cycle. Later maintenance treatment consisted mainly of sintilimab 200 mg. The treatment was individualized by the multidisciplinary team and did not follow a standard Ewing sarcoma regimen.

Serial CT examinations in March, June, August, and November 2024 and January 2025 showed no definite disease progression. Postoperative CT showed persistent soft-tissue density in the right nephrectomy bed but no clearly enlarging or progressively enhancing mass (**Figure 3D**). The patient had no worsening clinical symptoms, and routine serum tumor markers remained negative.

In May 2025, 21 months after surgery, follow-up ^{18}F-FDG PET/CT was performed. After fasting, 311 MBq (8.4 mCi) of ^{18}F-FDG was injected intravenously. Standard torso imaging began 66 minutes after injection; delayed abdominal imaging was obtained at 186 minutes, 120 minutes after the start of standard imaging. Nodular FDG uptake was present in soft tissue in the right nephrectomy bed, with SUVmax 9.7 on standard imaging and 11.4 on delayed imaging (**Figure 4**). The finding was considered indeterminate, and local recurrence could not be excluded. CT showed no discrete progressively enhancing mass, no distant FDG-avid disease was present, and serial imaging showed only limited change. The multidisciplinary team therefore deferred immediate biopsy and continued imaging follow-up. Sintilimab maintenance continued through October 2025. An external review of CT performed on August 22, 2025, showed no definite progression compared with the May PET/CT.

Discussion

Primary renal ES/PNET is difficult to diagnose because its symptoms and imaging findings are nonspecific. Most reported patients are adolescents or young adults who present with abdominal or flank pain, hematuria, hypertension, or an incidentally detected mass [1-4]. Histologically, ES/PNET is a small round cell tumor. Diffuse

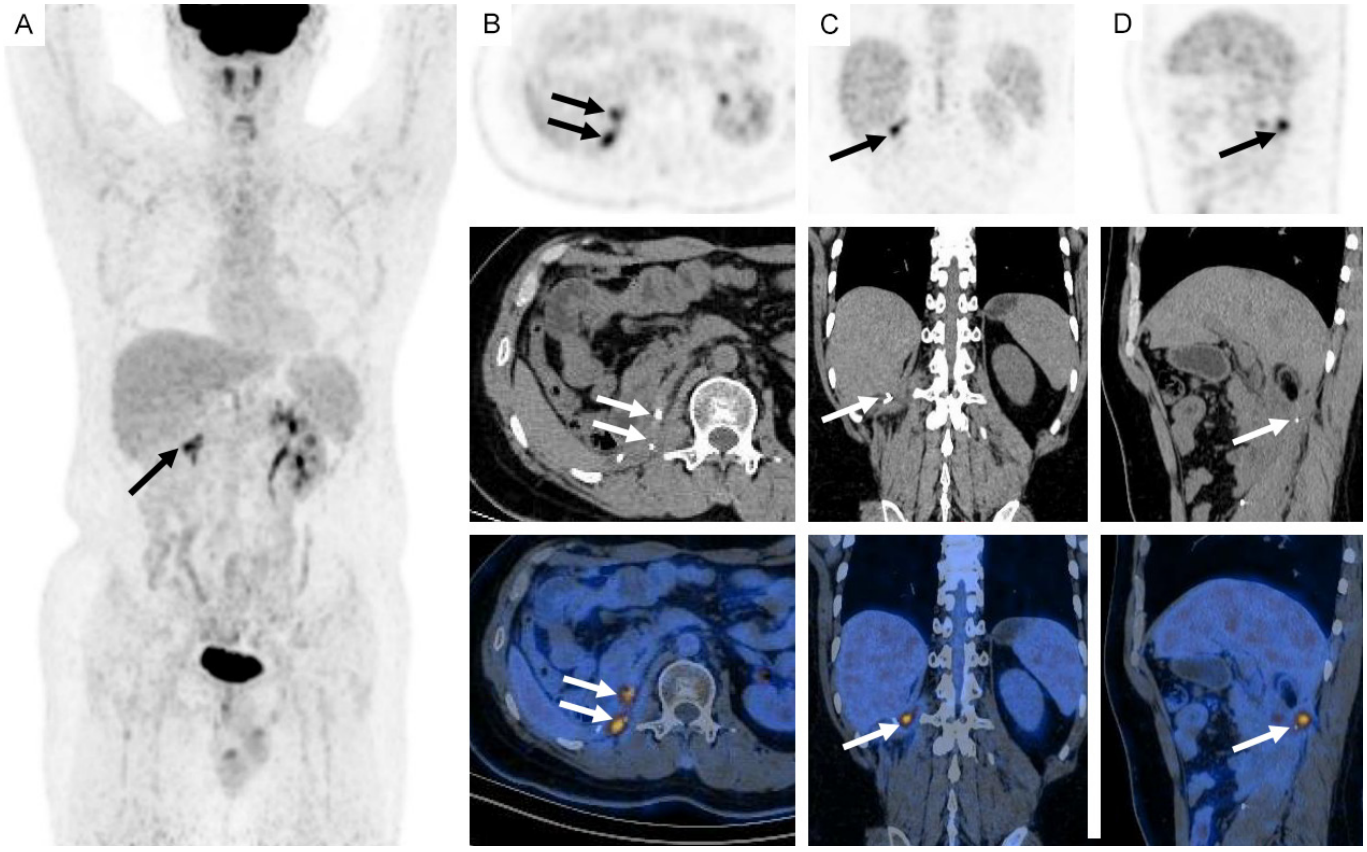


Figure 4. Follow-up PET/CT imaging findings. Follow-up ^{18}F-FDG PET/CT at 21 months after surgery shows nodular FDG uptake in the right nephrectomy bed (SUVmax 9.7 at 66 minutes and 11.4 at 186 minutes; delayed imaging was obtained 120 minutes after the start of standard imaging). (A) Coronal maximum intensity projection image shows the focus (arrow). (B) Axial, (C) coronal, and (D) sagittal PET/CT images localize the uptake to the surgical bed. The finding was considered indeterminate and was followed with serial anatomic imaging.

membranous CD99 expression is common, but immunohistochemistry alone is not specific because several renal and soft-tissue tumors can show similar findings. Molecular confirmation of an *EWSR1* rearrangement is useful when the morphology and immunophenotype are compatible with ES/PNET [1, 5, 6]. In this patient, detection of an *EWSR1-FLI1* rearrangement helped establish the diagnosis after the initial core biopsy showed a small round cell sarcoma.

The imaging findings in this patient, including large tumor size, mixed solid and cystic components, necrosis, and poorly defined margins, have been reported in renal ES/PNET [16-19]. These features overlap with renal cell carcinoma, renal lymphoma, angiomyolipoma with minimal fat, and Wilms tumor [20-25]. FDG uptake is also nonspecific: uptake in renal cell carcinoma varies by subtype and grade [20-22], renal lymphoma can be intensely FDG-avid [23], and adult Wilms tumor may present as a large heterogeneous renal mass [24]. PET/CT can assess disease extent and metabolic activity, but tissue diagnosis remains necessary.

^{18}F-FDG PET/CT combines whole-body staging with metabolic assessment in Ewing sarcoma. A systematic review reported good diagnostic performance for primary tumors, bone lesions, and recurrent disease [7], and cohort studies found associations between baseline or post-treatment PET findings and outcomes [8-10]. Evidence for primary renal ES/PNET is limited to case reports and small series. Published reports describe FDG-avid venous tumor thrombus, lymph node or distant metastases, and metabolic response during follow-up [11-15]. PET/CT may therefore complement CT or magnetic resonance imaging (MRI) for staging and surveillance. Reported cases of primary renal ES/PNET evaluated with ^{18}F-FDG PET or PET/CT are summarized in **Table 1**.

At baseline, PET/CT showed no FDG-avid distant disease and provided a baseline for comparison during follow-up. SUVmax in the solid component increased from 23.8 at 62 minutes to 32.7 at 120 minutes. The delayed increase in SUVmax was nonspecific and did not aid diagnosis.

Postoperative PET/CT showed an FDG-avid nodular focus in the surgical bed, whereas contrast-enhanced CT showed no discrete progressively enhancing mass. Although SUVmax increased from 9.7 to 11.4 on delayed imaging, uptake intensity and retention alone cannot distinguish recurrent tumor from postoperative or inflammatory change [26]. Recurrence therefore remained a con-

Table 1. Reported cases of primary renal ES/PNET evaluated with ^{18}F-FDG PET or PET/CT

Reference	Patient/primary lesion	Scan setting	Key FDG findings	Role of PET
Tripathy S, 2020 [11]	28-year-old man; left renal mass with IVC thrombus; size not reported	Initial staging	FDG-avid renal mass and IVC tumor thrombus; SUVmax not reported.	Defined venous tumor extension before nephrectomy.
Ozturk H, 2015 [12]	38-year-old woman; 6-cm left renal mass after nephrectomy	Restaging/response	A 17-mm para-aortic node not seen on CT had SUVmax 7.2; after first-line chemotherapy, it measured 14 mm with SUVmax 4.6; no metastatic focus was seen after second-line chemotherapy.	Detected CT-occult nodal metastasis and monitored response; no recurrence at 72 months.
Malhotra G, 2012 [13]	12-year-old boy; bilateral 4-5 cm renal masses with hepatic and pancreatic metastases	Baseline whole-body FDG PET/post-chemotherapy	Renal, hepatic, and pancreatic SUVmax values were 6.9, 7.2, and 5.4; intense marrow uptake produced a PET "super scan"; repeat PET showed marked metabolic response.	Showed extensive multiorgan and marrow disease and treatment response.
Doroudinia A, 2019 [14]	27-year-old woman; 69 × 60 × 95 mm right renal mass; peritoneal involvement	Restaging after chemotherapy	FDG-avid bilateral cervical, hilar, mediastinal, and retroperitoneal nodes; SUVmax not reported.	Showed systemic nodal metastatic disease.
Akhter P, 2023 [15]	28-year-old man; 13.6 × 14.5 × 12.8 cm left renal mass; chest imaging negative	Postoperative staging	FDG-avid abdominal nodes (SUVmax 15.7), peritoneal deposits (SUVmax 20.7), and multiple skeletal metastases.	Detected occult metastatic disease.

Abbreviations: ES/PNET, Ewing sarcoma/primitive neuroectodermal tumor; FDG, fluorodeoxyglucose; IVC, inferior vena cava; PET, positron emission tomography; CT, computed tomography; SUVmax, maximum standardized uptake value.

sideration. Because serial imaging showed only limited interval change and there was no progressively enlarging or enhancing lesion, distant FDG-avid disease, or clinical deterioration, the multidisciplinary team chose imaging surveillance rather than immediate biopsy. CT reviewed on August 22, 2025, showed no definite progression. The team planned to reconsider biopsy if the lesion enlarged or showed progressive enhancement, or if new metastatic disease or clinical progression occurred.

Treatment data for primary renal ES/PNET are limited, and management is generally extrapolated from Ewing sarcoma at other sites [2-4]. The treatment used in this patient was individualized and is reported only as part of the clinical course.

In this case, PET/CT was useful for initial staging and for localizing a postoperative FDG-avid focus. The postoperative finding, however, required correlation with contrast-enhanced CT and follow-up imaging.

Conclusions

Primary renal ES/PNET should be considered in the differential diagnosis of a large heterogeneous renal mass in a young adult, but confirmation requires pathological and molecular testing. In this case, ^{18}F-FDG PET/CT contributed to whole-body staging at presentation and localized an indeterminate postoperative focus during surveillance. FDG avidity in a surgical bed is not, by itself, evidence of recurrence and should be interpreted with anatomic imaging and interval change.

Acknowledgements

This work was supported by the National Natural Science Foundation of China (82472018, 82171970), Beijing Nova Program (20240484725), Beijing Municipal Science & Technology Commission (Z221100007422027), National Key Research and Development Program of China (2024YFE0113500), National High Level Hospital Clinical Research Funding (Interdisciplinary Research Project of Peking University First Hospital, 2023IR17, 2024IR07; Scientific and Technological Achievements Transformation Incubation Guidance Fund Project of Peking University First Hospital, 2025CX38, 2024CX18), Future Talent Development Plan in the Medical Engineering Field (MBZX202502-0029).

Written informed consent was obtained from the patient for publication of this case report and the accompanying clinical data and images.

Disclosure of conflict of interest

None.

Address correspondence to: Dr. Lei Kang, Department of Nuclear Medicine, Peking University First Hospital, No. 8 Xishiku Street, Xicheng District, Beijing 100034, China. Tel: +86-10-83575252; E-mail: kanglei@bjmu.edu.cn

References

[1] Jimenez RE, Folpe AL, Lapham RL, Ro JY, O'Shea PA, Weiss SW and Amin MB. Primary Ewing's sarcoma/primitive neuroectodermal tumor of the kidney: a clinicopathologic and immunohistochemical analysis of 11 cases. Am J Surg Pathol 2002; 26: 320-327.

[2] Hakky TS, Gonzalvo AA, Lockhart JL and Rodriguez AR. Primary Ewing sarcoma of the kidney: a symptomatic presentation and review of the literature. Ther Adv Urol 2013; 5: 153-159.

[3] Bradford K, Nobori A, Johnson B, Allen-Rhoades W, Naik-Mathuria B, Panosyan EH, Gotesman M, Lasky J, Cheng J,

Ikeda A, Goldstein J, Singh A and Federman N. Primary renal Ewing sarcoma in children and young adults. J Pediatr Hematol Oncol 2020; 42: 474-481.
[4] Hu X, Li D and Cai J. Experience of CT diagnosis and management of primary renal Ewing's sarcoma: a retrospective analysis of 6 cases and a literature review. Medicine (Baltimore) 2022; 101: e32189.
[5] Choi EY, Gardner JM, Lucas DR, McHugh JB and Patel RM. Ewing sarcoma. Semin Diagn Pathol 2014; 31: 39-47.
[6] Dehner LP. Primitive neuroectodermal tumor and Ewing's sarcoma. Am J Surg Pathol 1993; 17: 1-13.
[7] Seth N, Seth I, Bulloch G, Siu AHY, Guo A, Chatterjee R, MacManus M and Donnan L. 18F-FDG PET and PET/CT as a diagnostic method for Ewing sarcoma: a systematic review and meta-analysis. Pediatr Blood Cancer 2022; 69: e29415.
[8] Jamet B, Carlier T, Campion L, Bompas E, Girault S, Borrely F, Ferrer L, Rousseau M, Venel Y, Kraeber-Bodéré F and Rousseau C. Initial FDG-PET/CT predicts survival in adults Ewing sarcoma family of tumors. Oncotarget 2017; 8: 77050-77060.
[9] Salem U, Amini B, Chuang HH, Daw NC, Wei W, Haygood TM, Madewell JE and Costelloe CM. 18F-FDG PET/CT as an indicator of survival in Ewing sarcoma of bone. J Cancer 2017; 8: 2892-2898.
[10] Sobic Saranovic DP, Nikitovic M, Saponjski J, Grozdic Milojevic I, Paripovic L, Saranovic D, Beatovic S and Artiko VM. Post-treatment FDG PET/CT predicts progression-free survival in young patients with small round blue cell tumors: Ewing sarcoma and PNET. Eur J Radiol 2020; 129: 109076.
[11] Tripathy S, Shamim SA, Chellapuram S, Barwad A and Rastogi S. Primary Ewing sarcoma/primitive neuroectodermal tumor of kidney with inferior vena cava thrombus: findings on 18F-FDG PET/CT. Clin Nucl Med 2020; 45: e103-e105.
[12] Ozturk H. Peripheral neuroectodermal tumour of the kidney (Ewing's sarcoma): restaging with 18F-fluorodeoxyglucose (FDG)-PET/CT. Can Urol Assoc J 2015; 9: E39-E44.
[13] Malhotra G, Swami A, Shah P, Mittal N, Gandhi SJ, Tiwari B, Jatale PV and Asopa RV. F-18 fluorodeoxyglucose positron emission tomography "super scan" in a patient of metastatic primitive neuroectodermal tumor of the kidney. Indian J Nucl Med 2012; 27: 115-118.
[14] Doroudinia A, Ahmadi S, Mehrian P and Pourabdollah M. Primary Ewing sarcoma of the kidney. BMJ Case Rep 2019; 12: bcr-2018-227198.
[15] Akhter P, Mandal T, Mutsuddy P, Siddique MAB and Begum SMF. Role of 18F-FDG PET-CT imaging in a patient with renal Ewing's sarcoma: a rare case report. Bangladesh J Nucl Med 2023; 26: 54-57.
[16] Lee H, Cho JY, Kim SH, Jung DC, Kim JK and Choi HJ. Imaging findings of primitive neuroectodermal tumors of the kidney. J Comput Assist Tomogr 2009; 33: 882-886.
[17] Qian X, Kai X, Shaodong L, Gaohong C, Hong M and Jingjing L. Radiological and clinicopathological features of pPNET. Eur J Radiol 2013; 82: e888-e893.
[18] Khong PL, Chan GC, Shek TW, Tam PK and Chan FL. Imaging of peripheral PNET: common and uncommon locations. Clin Radiol 2002; 57: 272-277.
[19] Tan Y, Zhang H, Ma GL, Xiao EH and Wang XC. Peripheral primitive neuroectodermal tumor: dynamic CT, MRI and clinicopathological characteristics--analysis of 36 cases and review of the literature. Oncotarget 2014; 5: 12968-12977.
[20] Liu Y. The place of FDG PET/CT in renal cell carcinoma: value and limitations. Front Oncol 2016; 6: 201.
[21] Kim D, Lee N, Lee SH, Kim HJ, Hong HS, Park JS, Cho NH, Choi YD, Ham WS, Lee SH, Han WK and Yun M. Metabolic tumour volume on 18F-FDG PET/CT predicts extended pathological T stages in patients with renal cell carcinoma at staging. Sci Rep 2021; 11: 23486.
[22] Zhao Y, Wu C, Li W, Chen X, Li Z, Liao X, Cui Y, Zhao G, Liu M and Fu Z. 2-[18F]FDG PET/CT parameters associated with WHO/ISUP grade in clear cell renal cell carcinoma. Eur J Nucl Med Mol Imaging 2021; 48: 570-579.
[23] Nicolau C, Sala E, Kumar A, Goldman DA, Schoder H, Hricak H and Vargas HA. Renal masses detected on FDG PET/CT in patients with lymphoma: imaging features differentiating primary renal cell carcinomas from renal lymphomatous involvement. AJR Am J Roentgenol 2017; 208: 849-853.
[24] Wu J, Zhu Q, Zhu W and Chen W. CT and MRI imaging features and long-term follow-up of adult Wilms' tumor. Acta Radiol 2016; 57: 894-900.
[25] Xie J, Wen J, Bi YL and Li HZ. Primitive neuroectodermal tumour of the kidney: an unusual case mimicking renal angiomyolipoma with minimal fat. Can Urol Assoc J 2015; 9: E337-E339.
[26] Kinahan PE and Fletcher JW. Positron emission tomography-computed tomography standardized uptake values in clinical practice and assessing response to therapy. Semin Ultrasound CT MR 2010; 31: 496-505.